EC PROJECT
EVG1-CT-2002-00069

REL. I. E. F.

RELiable Information on Earthquake Faulting

Large Earthquake Faulting and Implications for the Seismic Hazard Assessment in Europe:

The Izmit-Duzce earthquake sequence of August-November 1999 (Turkey, Mw 7.4, 7.1)

Potential of vulnerability and seismic risk

Deliverable no. 27

January 2006

WP 6: Integration of multidisciplinary data for seismic hazard assessment
WP 9: Multidisciplinary seismic hazard assessment

Prepared by K. Atakan and M. B. Sørensen

PARTNER 6: Institutt for Geovitenskap, Universitetet i Bergen

List of Contents

Summary

Within the framework of workpackage 6 (WP06) of the RELIEF project, and as a part of workpackage 9 (WP09), seismic hazard assessment is performed using probabilistic and deterministic approaches. The final aim for these hazard studies is to implement the results in seismic risk assessment. In this report, seismic risk is calculated in terms of the estimated damage at the recently installed Istanbul Earthquake Early Warning and Rapid Response System (IEEWRRS) station sites.

Ground motion is simulated for the Rapid Response station sites using hybrid techniques as documented in previous deliverables (see RELIEF UiB Deliverables 25 and 26). These results are then combined with the existing vulnerability functions for the building categories, and damage maps are produced showing the distribution of collapsed buildings based on a scenario earthquake (M=7.5) in the Marmara Sea.

1. Introduction

Istanbul, with a population exceeding 12 millions, is considered one of the world's mega cities exposed to significant earthquake hazard. The disastrous consequences of the two large earthquakes in Izmit and Düzce in 1999 have highlighted the need for careful analysis of seismic hazard including local site effects, although the earthquake hazard in this region has been a topic of considerable interest for a long time. Recent results from several studies (e.g. Atakan et al., 2002; Erdik et al., 2003a; Erdik et al., 2004; Pulido et al., 2004), as well as the results presented in RELIEF deliverables 18, 25 and 26, show significant seismic hazard and emphasize the importance of earthquake preparedness and risk mitigation in the Istanbul metropolitan area and its rapidly growing surroundings.

As a response to this growing awareness of seismic hazard and risk in Istanbul, there are a number of earthquake risk mitigation efforts that are being implemented. One of these initiatives is the preparation of the Earthquake Master Plan for Istanbul (IBB, 2003). As a results of this a number of mitigation plans are being implemented such as the pilot microzonation study for the Zeytinburnu district, strengthtening of the school and hospital buildings, etc. Another important initative is the installation of the Istanbul Earthquake Early Warning and Rapid Response System (IEEWRRS) (Erdik et al., 2003b) by the Bogazici University, Kandilli Observatory and the Earthquake Research

Institute (KOERI). The system, which consists of 100 strong motion and ten broad-band stations, aims to provide rapid shake-maps and maps with expected damage distributions in Istanbul after each significant earthquake.

The main objective of the present study is to contribute to the detailed understanding of the seismic hazard in Istanbul and its consequences. The work starts with providing realistic ground motion simulations based on a future scenario earthquake in the Marmara Sea utilizing the recorded ground motion at the Rapid Response System (RRS is part of the IERREWS) stations in Istanbul. Two recent earthquakes that occurred on May 16, 2004 (Mw=4.2) and on Sept. 29, 2004 (Mw=4.1), recorded at the RRS stations, are used as Green's functions assuming that they represent parts of the target fault. Final goal of the present study is to demonstrate the effects of using a realistic scenario input from ground motion simulations to produce shake-maps and damage estimates.

2. Earthquake preparedness and risk mitigation strategies in Istanbul

There are a number of ongoing efforts in Istanbul aiming to improve earthquake prearedness and risk mitigation. In the following, two recent examples are explained in some detail. The first one of these is a joint effort on the Earthquake Master Plan for Istanbul (IBB, 2003) by the Istanbul Metropolitan Municipality and the four major Universities in Turkey. Three of these the Bogazici University (BU), Yildiz Technical University (YTU), and Istanbul Technical University (ITU) are located in Istanbul and the fourth, the Middle East Technical University (METU) is located in Ankara. The second is the recently installed Istanbul Earthquake Early Warning and Rapid Response System - IEEWRRS (Erdik et al., 2003b).

2.1. The Earthquake Master Plan for Istanbul

The Earthquake Master Plan for Istanbul (IBB, 2003) is a comprehensive study that addresses the earthquake hazard and risk in Istanbul and possible mitigation measures that can be considered. The analyses are conducted by two different teams (BU-YTU and ITU-METU) and the resuts are compiled in a detailed report. In the report, a "Current Situation" analysis is conducted that summarizes previous studies and provides a comprehensive summary of the risk to the population, buildings, transportation systems, and lifelines as well as the potential impact on essential facilities, services and emergency response. Seismic assessment of the existing inventory of buildings, their evaluation and strengthening are discussed. Several methods are proposed for the evaluation of the buildings. A discussion is provided related to legal issues pertaining to collection of information on the building characteristics. In a separate chapter, the report discusses issues related to the planning, legal issues, administration and finance. The report provides essentially two approaches for integration of risk reduction in urban planning and urban renovation of Istanbul. It discusses the legal and institutional arrangements and proposes new organizational structures to facilitate the implementation of the master plan. It also discusses various financial instruments for funding. Specific hardware and software, data structures and the related information management are also outlined in the report. The educational and social issues are considered and various earthquake preparedness programs, with an emphasis on community education and social networking, are proposed. Finally the report also consists of a disaster management and suggests a framework for emergency management for Turkey that provides a role to the provincial and local governments.

2.2. Istanbul Earthquake Early Warning System and Rapid Response System (IEEWRRS)

Bogazici University, Kandilli Observatory and Earthquake Research Institute (KOERI) in collaboration with the Governorate of Istanbul, First Army Headquarters and Istanbul Metropolitan Municipality, have recently installed the Istanbul Earthquake Early Warning and the Rapid Response System (IEEWRRS) (Erdik et al., 2003b). The system aims to provide reliable information in case of a significant earthquake in the region. The Rapid Response System (RRS) part of the IEEWRRS is composed of 100 strong motion stations (Figure 2.2.1) and is designed to provide shake, damage and casualty maps immediately after an earthquake for rapid response purposes. In addition, there are ten broad-band stations installed mainly in the eastern part of the Marmara Sea region, which constitute the Early Warning System (EWS) part of the IEEWRRS. The main aim of the EWS is to provide rapid information about the earthquake source parameters and issue early warning to relevant authorities.

Since its installation, the RRS has recorded two significant earthquakes on May 16, 2004 and September 29, 2004 with magnitudes (Mw) 4.2 and 4.1, respectively. Both earthquakes are located along the North Boundary fault (Figure 2.2.2), which is a releasing bend of the North Anatolian Fault Zone (NAFZ) in the Marmara Sea. The source parameters of these earthquakes are given in Table 1, together with other significant (M>4) earthquakes that have occurred since 1999. Seismograms from the May 16, 2004 earthquake as recorded by the RRS stations are shown in Figure 2.2.3. The focal mechanism of the May 16, 2004 earthquake (Event #6 in Table 1) has been determined by a moment tensor solution with reasonable fit at eight station records (Figure 2.2.3). The resulting solution indicates an oblique-normal focal mechanism, with a second nodal plane that agrees well with the strike orientation, dip and the expected slip of the North Boundary fault. The location of this event, however, falls close to the intersection with the Hersek segment of the NAFZ, where the dominant mechanism expected is pure strike-slip (right-lateral). The oblique-normal faulting indicates clearly that the earthquake have occurred along the SE-edge of the North Boundary fault and not on the offshore Westward extension of the Hersek segment of the NAFZ.

Table 1: Source parameters of significant earthquakes in the Marmara Sea since 1999 (data from KOERI-National Earthquake Observation Center UDIM). Note that only events # 6 and 7 are used in the study since these are the only significant earthquakes recorded by the IERREWS since its installation in 2003.

Event #	Date	Time (UTC)	Location		Depth (km)	Mag. Mw	Focal mechanism			
			Latitude (deg. N)	Longitude (deg. E)			V	Ø	δ	λ
1	20.09.1999	21:27:59	40.69	27.58	16.0	4.8	m	245	40	166
2a	20.10.1999	23:08:21	40.79	29.00	10.6	4.4	m	293	73	164
2b	20.10.1999	23:08:21	40.79	29.00	8.0	4.9	f	32	71	16
3	24.03.2001	13:07:39	40.84	28.83	11.0	3.7	m	106	87	-160
4	28.02.2002	08:37:51	40.824	28.121	11.5	4.8	f	072	60	162
5	23.03.2002	02:36:10	40.844	27.852	13.8	4.8	f	274	60	-165
6	16.05.2004	03:30:48	40.712	29.340	13.0	4.2	f	128	80	-135
							m	151	54	-152
7a	29.09.2004	17:42:07	40.784	29.036	14.0	4.1				
7b	29.09.2004	17:42:07	40.810	29.050	10.0		f	159	22	0

Mw: Moment magnitude
V: Version (f: first motion polarities; m: moment tensor solution)
Ø: Strike angle in degrees
δ: Dip angle in degrees
λ: Slip angle in degrees
1, 2b, 3: Pinar et al., (2003)
2a: Örgülü et al., (2001)
4, 5, 6, 7a: KOERI-UDIM
7b: This study

The location of the second event (Event #7 in Table 2) on September 29, 2004, is definitely on the North Boundary fault as it falls in the area just south of the Princess Islands (Figure 2.2.2). In this case the trials with the moment tensor inversion did not give satisfactory results. However, we believe that the focal mechanism of this event is probably very similar to the May 16, 2004 earthquake because of its location. Further evidence for this comes from a recent OBS survey conducted in the Marmara Sea (Sato et al., 2004). The composite focal mechanism obtained for the small earthquakes that occurred in the same area agrees well with the mechanism obtained for the May 16, 2004 event. In the table above the focal mechanism for the Sept. 29 event is included as it was reported by the KOERI-UDIM.

The recorded ground motion distributions from these two earthquakes are shown in Figure 2.2.4. These two events, although small in size, are probably representative for the SE-part of the North Boundary fault and can be used for further ground motion simulations as Green's functions.

Along the same segment of the NAFZ (North Boundary fault), a previous earthquake with a surface-wave magnitude of 6.4 occurred on September 18, 1963 (McKenzie, 1972; Taymaz et al., 1991). The location of this event is not very reliable due to the lack of dense instrumental networks in the region at the time. However, based on the macroseismic observations and the available instrumental records, the location of the event is probably at the SE-part of the North Boundary fault associated with the area bounded by the two events that occurred in 2004 (Events # 6 and #7).

3. Seismic hazard analysis for IEEWRRS

Seismic hazard analysis for the IEEWRRS is conducted using the hybrid ground motion simulation methodology which is explained in detail in RELIEF Deliverables 25 and 26. In the following, ground motion simulation results are presented for the bedrock conditions using a similar input as the one used in the paper by Pulido et al., (2004). In addition, there is an ongoing effort to assess the site effects for each Rapid Response (RRS) station site. The preliminary results from this is given briefly, which is based mainly on the work conducted by colleagues at the Kandilli Observatory and Earthquake Research Institute (KOERI) of Bogazici University, Istanbul. Once these studies on the site effects assessment on all RRS station sites are finalized, the ground motion simulations will be extended accounting also for the site effects. However, this is outside the scope of the RELIEF Project. The prupose of this section is to demonstrate the potential seismic risk in Istanbul by providing a set of ground motion simulation results which are used as input to the risk calculations. These results are then combined with the vulnerability functions established for different building categories in estimating the damage. The damage is expressed in terms of collapsed buildings.

3.1. Ground motion simulations for the bedrock conditions

Ground motion simulations are performed for all the RRS stations assuming bedrock conditions using the methodology applied in Pulido et al. (2004). Broadband frequency (0.1 – 10 Hz) bedrock strong ground motion simulations are based on a fault rupture scenario and a source asperity model. The technique combines a deterministic simulation of seismic wave propagation at low frequencies with a semi-stochastic procedure for the high frequencies. To model the high frequencies, we applied a frequency-dependent radiation pattern model, which efficiently removes the effective dependence of the pattern coefficient on the azimuth and take-off angle as the frequency increases.

The idea is to evaluate the strong ground motion radiated from a finite fault, multi-asperity source model. The total ground motion radiated at each asperity is obtained by adding the low-frequency and high-frequency waveforms in time domain. Details of the simulation technique are explained in Pulido and Kubo (2004) and Pulido et al., (2004).

For the low-frequency (0.1 to 1 Hz) ground motion, asperities are subdivided into several point sources, and the time delayed ground motions from them is added, assuming a random or a constant rupture velocity. The seismogram from each point source is obtained numerically by the discrete wave number method of Bouchon (1981), which computes wave propagation in a flat-layered velocity structure, for a particular focal mechanism and source time function.

The high-frequency (1 to 10 Hz) ground motion is again calculated for finite asperities consisting of several subfaults. The ground motion from each subfault is obtained using a technique based on the stochastic approach of Boore (1983), summation being performed by the empirical Green's function method (Irikura, 1986), which is very efficient for radiation at high frequencies from finite faults. Boore's (1983) procedure was modified by Pulido and Kubo (2004), by introducing a frequency dependent radiation pattern into the ground motion acceleration spectrum.

The earthquake scenario considered consists of the rupture of the closest segments of the North Anatolian Fault System to the city of Istanbul. Our scenario earthquake involves the rupture of the entire North Anatolian Fault beneath the Sea of Marmara, namely the combined rupture of the Central Marmara Fault and North Boundary Fault segments. The fault rupture scenario is based on two asperities, one located within the Central Marmara Fault on the easternmost section before the bending point, and the other located within the continuation at the western section of the North Boundary fault. The fault and asperity parameters for the scenario were determined from empirical scalings and from results of kinematic and dynamic models of fault rupture. This model scenario corresponds roughly to the "scenario 1a" at Pulido et al. (2004), with minor modifications. The rupture initiation point is assumed to be at the westernmost end of the Central Marmara fault and is critical for the distribution of the ground motion in southern Istanbul with its dense population, especially taking into account the directivity effects.

The broad-band ground motions at RRS station locations are calculated in time series and spectra. The results are presented in color-shaded contour maps showing the ground motion distribution at the RRS station locations corresponding to peak ground accelerations and peak ground velocities (Figure 3.1.1). The distribution of the PGV values (cm/sec) gave somewhat better representation of the ground motion distribution than the PGA values (in cm/sec^2), which suffer probably from interpolation problems. However, the ground motion distribution in general follows the expected pattern similar to the distribution obtained by the computations on a regular grid (Pulido et al., 2004). The simulated ground motions indicate large values of acceleration response spectra at long periods, which could be critical for building damage at Istanbul during an actual earthquake.

3.2. Ground motion simulation results for the Rapid Response Station sites

We have performed also ground motion simulations using a scenario based on the rupture along the North Boundary Fault (NBF) alone. In this scenario, the recordings of the May 16, 2004 (Mw=4.2) event are used as an Empirical Green's Functions (EGF) for an asperity located close to the easternmost end of the fault. The magnitude of the scenario event is 7.1 based on the Sommerville et al. (1999) relation using 45 x 20 km fault area. The length of the NBF is well constrained by the bathymetry of the northern escarpment of the Cinarcik basin, however, the depth of the seismogenic zone is uncertain. The assumed depth of 20 km is based on the hypocentral depths of the small and moderate size earthquakes that occur in the Marmara Sea region (e.g. Gürbüz et al., 2000; Pinar et al., 2003; Sato et al., 2004).

Table 2: Fault and asperity parameters of the scenario earthquake along the North Boundary Fault (NBF). The three possible solutions for the geometry and mechanism of NBF is given together with the size of the asperities and the moment used in the Empirical Green's Function (EGF).

Fault Parameters	M_O (Nm)	$\Delta\sigma$ (bars)	# sub-faults	Fault dimensions (in km)		M_W	Fault geometry and mechanism			Asperity depth (in km)
				Length	Width		Ø	δ	λ	
Entire NBF (a)	6.183×10^{19}		369	45	20	7.1	106	64	-146	
Version (b)							110	90	-135	
Version (c)						5.2	112	88	170	
Asperity # 2	2.473×10^{19}	100	225	15	15					3
Background # 4	3.710×10^{19}	50	144							
EGF	2.076×10^{15}					4.2				

Mw: Moment magnitude
M_O : Seismic moment
$\Delta\sigma$: Stress-drop
Focal mechanism versions: (a) Composite solution from Sato et al. (2004) (b) solution used in the previous simulations (Pulido et al., 2004) (c) Solution for the Aug.17, 1999 Mw=5.2 earthquake (Pinar et al., 2003)

Ø: Strike angle in degrees
δ: Dip angle in degrees
λ: Slip angle in degrees

The ground motion simulation parameters used in this scenario are given in Table 2. In this scenario, we assume an asperity along the westernmost end of the fault located 3 km from the surface. The dimensions of the asperity are adjusted using 0.25 for the ratio of the asperity/fault area, which corresponds to 15x15 km^2. This value is similar to the global average of 0.22 (Somerville et al., 1999). The focal mechanism of the May 16, 2004 earthquake (Table 1) is compatible with the tectonics of the area where the regional stress-tensor with σ_1 oriented NW-SE and σ_3 oriented NE-SW (Pinar et al., 2003) produces oblique-normal faulting with a significant right-lateral component along the NBF. Regarding the geometry of the NBF at depth however, Okay et al. (2000), have proposed a southwestward dipping normal fault following the escarpment morphology, which at depth becomes near vertical. The proposed change in the dip of the fault is suggested to be around 3-4 km depth. The focal mechanism of a number of events along the NBF suggest pure strike-slip faulting, which is compatible with Okay et al.'s (2000) interpretation. More recently however, Sato et al., (2004) have computed a composite focal mechanism based on OBS data using moment tensor inversion, and found an oblique normal faulting with a significant right-lateral strike-slip component. Both these solutions have similar hypocentral depths around 10 km. In our simulations we have used the latter solution from Sato et al., (2004) for simplicity. Introducing a changing dip angle in the computations would produce additional uncertainties and at this stage we feel that our knowledge of the fault geometry at depth is not sufficient to resolve this.

Two examples of simulated seismograms and spectra are shown in Figures 3.2.1 and 3.2.2. In general the level of ground motions are slightly lower when compared to the results presented in the previous section where an earthquake scenario using a simultaneous rupture of the NBF and CMF segments.

3.2.1. Site effects for the IEEWRRS stations

Previous studies of local site effects, following the 1999 Izmit and Düzce earthquakes, have focused mainly on the Avcilar district of western Istanbul (e.g. Özel et al., 2002; Tezcan et al., 2002), and on the city of Adapazari in the east (e.g. Bakir et al., 2002; Komazawa et al., 2002; Sancio et al., 2002; Beyen and Erdik 2004 and Ansal et al., 2004), which experienced significant damage mainly due to site effects. In both areas, the presence of soft sediments in basin structures has caused strong amplifications of earthquake ground motions during past earthquakes.

As for the city of Istanbul, possible effects of local geological variations have been studied in several microzonation studies (e.g. JICA, 2004; Eyidogan et al., 2000; Ansal et al., 2004). The geological map showing the distribution of main units indicates that there are significant differences in both the age and the composition of these units (Figure 3.2.3). Birgören et al. (2004) found amplification levels up to a factor of 7 for some geological formations at 1 and 3 Hz frequencies, based on spectral ratios of records from a M=4.2 earthquake (Figure 3.2.4 and 3.2.5). More recently, Sørensen et al. (in review), have studied the local site effects at Ataköy using a 3-D FD-scheme. Their results indicate that there exist clear amplifications along the alluvial and fluvial deposits associated with the N-S oriented river systems. They found these amplifications to be at frequencies around 3-5 Hz and in addition, they infer amplifications (though less significant) around 1 Hz which are attributed to the response of the Bakirköy and Güngören formations.

In order to estimate the site effects at all RRS station sites, a comprehensive microtremor survey was conducted (Özel et al., 2005). The results from this study are shown in Figures 3.2.6 and 3.2.7. In general, "clear-peaks" (following the definition suggested by Bard et al., 2004) observed on some of the sites agree with the standard spectral ratios observed on the 16 May 2004 (Mw=4.2) earthquake record. The peaks observed around 1.0 – 1.5 Hz are probably associated with the Bakirköy formation. This is in agreement with results that were obtained in previous studies (e.g. Eyidogan et al., 2000; Sørensen et al., in review).

4. Seismic risk

In order to provide an overview of the possible damage due to a scenario earthquake, the ground motion simulations are computed for the IEEWRRS station sites and then converted to response spectra. The scenario used is the one described in section 3.2, where we simulate ground motions due to a M=7.1 earthquake along the NBF using EGF. Figures 4.1 – 4.4 show the spatial distribution of PGA (Figure 4.1.1) and response spectral displacements in three frequency bands for 1-3 Hz (Figure 4.2), 3-5 Hz (Figure 4.3) and f>5 Hz (Figure 4.4). These results are used as the hazard input to risk computations, by combining with the vulnerability functions established for different building categories. The chosen frequency ranges correspond roughly to the most common height categories of building stock in Istanbul (i.e. 1-4 floors "low-rise", 5-8 floors "mid-rise" and >8 floors "high-rise" buildings). The vulnerability functions and the methods of damage computations based on rectangular cells are developed by KOERI. In this report we applied the same building inventory and methods for estimating the vulnerability functions. The results are presented in terms of collapsed buildings in each cell.

4.1. Damage maps for Istanbul based on ground motion simulations

Based on the ground motion simulations, a damage distribution map is produced using the already established IEEWRRS procedures. The results are presented in terms of collapsed buildings in a grid of cells (Figure 4.1.1). The distribution clearly shows that there is a significant risk posed on several locations within the metropolitan area of Istanbul. The highest values are obtained in locations where both hazard and the vulnerability functions are high. Examples are locations such as Fatih and Zeytinburnu, which have dense building structure and relatively high vulnerability functions. In genral it can be seen that the total number of collapsed buildings is much larger in the SW part of the city on the European side when compared to the SE part on the Asian side. Clearly the damage is gradually reduced when moving towards north.

5. Concluding remarks

Results presented in this report should be considered as preliminary and are meant as a pilot study for demonstrating the effects of ground motion simulations on damage. The intention here is to establish routines than can be used in more comprehensive risk analysis for the Istanbul area in the future. These preliminary results show clearly that the strong ground motion simulations based on realistic earthquake scenarios, when combined with vulnerability functions provide a good estimate of the expected level of risk in Istanbul. These results are important with regard to the ongoing efforts of risk mitigation in the metropolitan area in terms of strengthtening the critical buildings such as hospitals and schools as well as planning activities for future settlements in Istanbul.

Acknowledgements

The work presented in this report is carried out in close cooperation with several colleagues at the Department of Earthquake Engineering, Kandilli Observatory and Earthquake Research Institute (KOERI), of Bogazici University, Istanbul. We thank especially Mustafa Erdik, Eser Durukal, Oguz Özel, Gulüm Birgören and Yasin Fahjan. We also thank Nelson Pulido from NIED, Japan for his contributions in ground motion simulations. Needles to say, collaborations with the RELIEF Partners are also appreciated.

References

Ambraseys, N.N. 2002. The seismic activity of the Marmara Sea Region over the last 2000 years. *Bull. Seismol. Soc. Am.*, 92, 1-18

Ansal, A., Laue, J., Buchheister, J., Erdik, M., Springman, S.M., Studer, J. and Koksal, D.,2004. Site characterization and site amplification for a seismic microzonation study in Turkey, *Proceedings of the 11th Intl. Conf. on Soil Dyn. & Earthquake Engng. (11th ICSDEE) & the 3rd Intl. Conf. on Earthquake Geotech. Engng. (3rd ICEGE), January 7-9, Berkeley, CA*, pp. 53-60.

Aochi, H., and Madariaga, R. 2003. The 1999 Izmit, Turkey, Earthquake: Nonplanar Fault Structure, Dynamic Rupture Process, and Strong Ground Motion. *Bull. Seismol. Soc. Am.*, 93, 1249-1266.

Atakan, K., 1995. A review of the type of data and the techniques used in empirical estimation of local site response, *Proceedings of the "Fifth International Conference on Seismic Zonation", October 17-19, 1995, Nice, France*, Ouest Éditions, Presses Académiques, Vol. II, 1451-1460.

Atakan, K., Ojeda, A., Meghraoui, M., Barka, A.A., Erdik, M. and Bodare, A., 2002. Seismic hazard in Istanbul following the 17 August 1999 Izmit and 12 November 1999 Düzce earthquakes, *Bull. Seismol. Soc. Am*, 92, 466-482.

Atakan, K., Duval, A.-M., Theodulidis, N., Guillier, B., Chatelain, J.-L., Bard, P.-Y. and the SESAME-team, 2004a. The H/V spectral ratio technique: Experimental conditions, data processing and empirical reliability assessment, *Proceedings of the 13th World Conference on Earthquake Engineering, Vancouver, Canada, 1-6 August, 2004*, paper no. 2268.

Atakan, K., Bard, P-Y., Kind, F., Moreno, B., Roquette, P. and Tento, A. and the SESAME team, 2004b. J-SESAME: a standardized software solution for the H/V spectral ratio technique, *Proceedings of the 13th World Conference on Earthquake Engineering, Vancouver, Canada, 1-6 August, 2004*, paper no. 2270.

Bard, P-Y. et al. (including SESAME Project Participants). 2004. Guidelines for the Implementation of the H/V Spectral Ratio Technique on Ambient Vibrations: Measurements, processing and interpretation. SESAME Project Report. Universite Joseph Fourier, Grenoble, France. 50p.

Bakir, B.S., Sucuoglu, H. and Yilmaz, T., 2002. An overview of local site effects and the associated building damage in Adapazari during the 17 August 1999 Izmit earthquake, *Bull. Seismol. Soc. Am*, 92, 509-526.

Beyen, K. and Erdik, M., 2004. Two-dimensional nonlinear site response analysis of Adapazari plain and predictions inferred from aftershocks of the Kocaeli earthquake of 17 August 1999, *Soil Dynamics and Earthquake Engineering*, 24, 261-279

Birgören, G., Özel, O., Fahjan, Y. and Erdik, M., 2004. Determination of site effects in Istanbul area using a small earthquake record of the dense strong motion network, *XXIX General Assembly of the European Seismological Commision, Potsdam, Germany*, poster no. 249.

Bonnefoy-Claudet, S., Cornou, C., Kristek, J., Ohrnberger, M, Wathelet, M., Bard, P.-Y., Moczo, P., Faeh, D. and Cotton, F., 2004. Simulation of seismic ambient noise: I. Results of H/V and array techniques on canonical models, *Proceedings of the 13th World Conference on Earthquake Engineering, Vancouver, Canada, 1-6 August, 2004*, paper no.1120.

Boore, D. M., 1983. Stochastic simulation of high frequency ground motions based on seismological models of the radiated spectra, *Bull. Seismol. Soc. Am.*, 73, 1865-1894.

Bouchon, M., 1981. A simple method to calculate Green's functions for elastic layered media, *Bull. Seismol. Soc. Am.*, 71, 959-971.

Cerjan C., Kosloff R. and Reshef M., 1985. A nonreflecting boundary condition for discrete acoustic and elastic wave equations, *Geophysics*, 50, 705-708.

Chatelain, J-L., Guillier, B., Duval, A-M., Cultrera, G., Cara, F., Teves-Costa, P., Atakan,K., and Bard, P-Y., in prep. Evaluation of the influence of experimental conditions on H/V results from ambient noise recordings. To be submitted to *Bulletin of Earthquake Engineering.*

Duval, A.-M., Bard, P.-Y., Méneroud, J.-P. and Vidal, S., 1994. Usefulness of microtremor measurements for site effect studies, *proceedings of the 10th European Conference on Earthquake Engineering, Vienna, Austria*.

Duval, A.-M., Bard, P.-Y., Méneroud, J.-P. and Vidal, S., 1995. Mapping of site effects with microtremors, *Proceedings of the Fifth International Conference on Seismic Zonation, Nice, October 1995*.

Emerman S.H. and Stephen R.A., 1983. Comment on Absorbing Boundary Conditions for Acoustic and Elastic wave Equations, by R. Clayton and B. Enquist, *Bull. Seismol. Soc. Am.*, 73, 661-665.

Erdik, M., Aydinoglu, N., Fahjan, Y., Sesetyan, K., Demircioglu, M., Siyahi, B., Durukal, E., Ozbey, C., Biro, Y., Akman, H. and Yuzugullu, O., 2003a. Earthquake risk assessment for Istanbul metropolitan area, *Earthquake Engineering and Engineering Vibration*, Vol. 2, No. 1, 1-25.

Erdik, M., Fahjan, Y., Özel, O., Alcik, H., Mert, A., and Gül, M. 2003b. Istanbul Earthquake Rapid Response and the Early Warning System. *Bulletin of Earthquake Engineering* 1, 157-163.

Erdik, M., Demircioglu, M., Sesetyan, K., Durukal, E. and Siyahi, B., 2004. Earthquake hazard in Marmara region, Turkey, *Proceedings of the 11th SDEE/ 3rd ICEGE, California, USA.*

Eyidogan, H., Ecevitoglu, B. and Caglar, I., 2000 (in Turkish). Bakirköy Ilcesi 1. etap (Bakirköy-Ataköy) yerlesim alanlarinin jeolojik yapi ve depremsellik etüdü projesi, *Internal Report*, part 6, TC. Bakirköy Belediyesi and ITÜ Gelistirme Vakfi. 55 p.

Fäh, D., Rüttener, E., Noack, T. and Kruspan, P., 1997. Microzonation of the city of Basel, *Journal of Seismology*, 1, 87-102.

Field, E.H. and Jacob, K., 1993. The theoretical response of sedimentary layers to ambientseismic noise, *Geophysical Research Letters*, 20(24), 2925-2928, 10.1029/93GL03054.

Field, E.H., Clement, A.C., Jacob, K.H., Ahronian, V., Hough, S.E., Friberg, P.A., Babaian, T.O., Karapetian, S.S., Hovanessian, S.M. and Abramian, H.A., 1995. Earthquake site-response study in Giumri (formerly Leninakan), Armenia, using ambient noise observations, *Bull. Seismol. Soc. Am.*, 85, 349-353.

Gitterman, Y., Zaslavsky, Y., Shapira, A. and Shtivelman, V., 1996. Emperical site response evaluations: case studies in Israel, *Soil Dynamics and Earthquake Engineering*,15, 447-463.

Guillier, B., Atakan, K., Chatelain, J-L., Havskov, J., Duval, A-M., Ohrnberger, M., Cara, F., and Zacharapoulous, S., in prep. Influence of instruments on the H/V spectral ratios of ambient vibrations. To be submitted to *Bulletin of Earthquake Engineering*.

Gurbuz, C., M. Aktar, H. Eyidogan, A. Cisternas, H. Haessler, A. Barka, M. Ergin, N. Turkelli, O. Polat, S. B. Ucer, S. Kuleli, S. Baris, B. Kaypak, T. Bekler, E. Zor, F. Bicmen, and A. Yoruk. 2000. The seismotectonics of the Marmara region (Turkey): results from a microseismic experiment, *Tectonophysics* 316, 1-17.

Harris, R. A., R. J. Archuleta, and S. M. Day. 1991. Fault Steps and the Dynamic Rupture Process - 2-D Numerical Simulations of a Spontaneously Propagating Shear Fracture, *Geophys. Res. Lett.* 18, 893-896.

Harris, R. A., and S. M. Day. 1993. Dynamics of Fault Interaction - Parallel Strike-Slip Faults, *J. Geophys. Res.* 98, 4461-4472.

Harris, R. A., and S. M. Day. 1999. Dynamic 3D simulations of earthquakes on en echelon faults, *Geophys. Res. Lett.* 26, 2089-2092.

Hisada, Y., 1994. An efficient method for computing Green s functions for a layered half-space with sources and receivers at close depths, *Bull. Seismol. Soc. Am.*, 84, 1456-72.

IBB. 2003. Earthquake Master Plan for Istanbul. Metropolitan Municipality of Istanbul, Turkey. 1300p.

Ibs-von Seht, M., and Wohlenberg, J. 1999. Microtremor measurements used to map thickness of soft sediments. *Bull. Seismol. Soc. Am.*, 89, 250-259.

Irikura, K., 1986. Prediction of strong acceleration motion using empirical Green's function, *Proceedings of the 7th Japan. Earthq. Eng. Symp.*, 151-156

Japan International Cooperation Agency (JICA) 2004. Country Strategy Paper for Natural Disasters in Turkey, JICA-Report, Turkiye Cumhuriyeti Icisleri Bakanligi, Ankara, July 2004, 154p.

Karabulut, H., Özalaybey, S., Taymaz, T., Aktar, M., Selvi, O., and Kocaoğlu, A. 2003. A tomographic image of the shallow crustal structure in the Eastern Marmara, *Geophysical Research Letters*, Vol. 30, No. 24, 2277-2280.

Kase, Y., and Kuge, K. 1998. Numerical simulation of spontaneous rupture processes on two non-coplanar faults: the effect of geometry on fault interaction, *Geophys. J. Int.* 135, 911-922.

Kase, Y., and Kuge, K. 2001. Rupture propagation beyond fault discontinuities: significance of fault strike and location, *Geophys. J. Int.* 147, 330-342.

Komazawa, M., Morikawa, H., Nakamura, K., Akamatsu, J., Nishimura, K., Sawada, S., Erken, A. and Onalp, A., 2002. Bedrock structure in Adapazari, Turkey a possible cause of severe damage by the 1999 Kociaeli earthquake, *Soil Dynamics and Earthquake Engineering*, 22, 829-836.

Kudo, K., 1995. Practical estimates of site response, State-of-the-art report, *proceedings of the Fifth International Conference on Seismic Zonation, Nice, October 1995.*

Lachet, C., and P.-Y. Bard, 1994. Numerical and theoretical investigations on the possibilities and limitations of the "Nakamura's" technique, *Journal of Physics of the Earth*, 42-4, 377-397.

Lachet, C., Hatzfeld, D., Bard, P.-Y., Theodulidis, N., Papaioannou, C. and Savvaidis, A., 1996. Site effects and microzonation in the city of Thessaloniki (Greece): comparison of different approaches, *Bull. Seismol. Soc. Am.*, 86, 1692-1703.

Lebrun, B., Bard, P.-Y. and Hatzfeld, D., 1997. Evidence for large, low frequency site effects in large alpine valleys: the example of Grenoble, France, *29th general assembly of IASPEI, Workshop W16, Thessaloniki, Greece*.

Le Pichon, X., A. M. C. Sengor, E. Demirbag, C. Rangin, C. Imren, R. Armijo, N. Gorur, N. Cagatay, B. M. de Lepinay, B. Meyer, R. Saatcilar, and B. Tok 2001. The active Main Marmara Fault, *Earth and Planetary Science Letters* 192, 595-616.

Lermo, J. and Chávez-García, F.J., 1993. Site effect evaluation using spectral ratios with only one station. *Bull. Seismol. Soc. Am.*, 83, 1574-1594.

Lermo, J. and Chávez-García, F.J., 1994. Are microtremors useful in site response evaluation? *Bull. Seismol. Soc. Am.*, 84, 1350-1364.

McKenzie, D. 1972. Active tectonics of the Mediterranean region. *Geophys. Journal of Royal Astronomical Society* 30, 109-185.

Mucciarelli, M., 1998. Reliability and applicability of Nakamura's technique using microtremors: An experimental approach, *J. Earthquake Eng*, 2, 1 14.

Mucciarelli, M., Gallipoli, M.R. and Arcieri, M., 2003. The stability of Horizontal-to-Vertical Spectral Ratio of triggered noise and earthquake recordings, *Bull. Seismol. Soc.Am.*, 93, 1407-1412.

Nakamura, Y., 1989. A method for dynamic characteristics estimation of subsurface using microtremors on the ground surface. *Quarterly Report of the Railway Technical Research Institute*, 30, 1.

Nakamura, Y., 2000. Clear identification of fundamental idea of Nakamura's technique and its applications, *Proceedings of the 12th WCEE, New Zealand*, paper no. 2656

Oglesby, D. D. 1999. Earthquake dynamics on dip-slip faults, Ph. D. Thesis, University of California, Santa Barbara.

Oglesby, D. D. 2005. The dynamics of strike-slip stepovers with linking dip-slip faults, *Bull. Seismol. Soc. Am.* in press.

Okay, A. I., A. Kashlar-Ozcan, C. Imren, A. Boztepe-Guney, E. Demirbag, and I. Kuscu. 2000. Active faults and evolving strike-slip basins in the Marmara Sea, northwest Turkey: a multichannel seismic reflection study, *Tectonophysics* 321, 189-218.

Oprsal, I., Brokesova, J., Faeh, D., and Giardini, D., 2002. 3D Hybrid Ray-FD and DWNFD Seismic Modeling For Simple Models Containing Complex Local Structures, *Stud.Geophys. Geod.*, 46, 711-730.

Oprsal, I. and Zahradnik, J., 2002. Three-dimensional finite difference method and hybrid modeling of earthquake ground motion, *J. Geophys. Res.*, 107(B8), DOI10.1029/2000JB000082.

Oprsal, I., Faeh, D., Mai, M. and Giardini, D., 2005. Deterministic earthquake scenario for the Basel area - Simulating strong motion and site effects for Basel, Switzerland, *J. Geophys. Res.*, 110, doi:10.1029/2004JB003188.

Özel, O., Cranswick, E., Meremonte, M., Erdik, M. and Safak, E., 2002. Site effects in Avcilar, west of Istanbul, Turkey, from strong- and weak.motion data, *Bull. Seismol. Soc.Am.*, 92, 499-508.

Özel, O., Birgören, G., Alcik, H. 2005. Natural frequencies of the sedimentary cover in Istanbul from weak-motion records and microtremor measurements. Poster presentation, Seismological Society of Japan 2005 Fall Meeting, Sapporo, Japan.

Parsons, T., Toda, S., Stein, R.S., Barka, A., and Dieterich, J.H. 2000. Hightened odds of a large earthquake near Istanbul. An interaction based probability calculation. *Science* 288, 661-665.

Peng, Z., and Ben-Zion, Y. 2005. Temporal changes of shallow seismic velocity around the Karadere-Düzce branch of the north Anatolian fault and strong ground motion. Submitted to the *Pure and Applied Geophysics*.

Pinar, A., Kuge, K., and Honkura, Y. 2003. Moment tensor inversion of recent small to moderate sized earthquakes: implications for seismic hazard and active tectonics beneath the Sea of Marmara. *Geophysical Journal International* 153, 133-145.

Pulido, N. and Kubo, T., 2004. Near-fault strong motion complexity of the 2000 Tottori earthquake (Japan) from a broadband source asperity model, *Tectonophysics*, 390, 177-192.

Pulido, N., Ojeda, A., Atakan, K. and Kubo, T., 2004. Strong ground motion estimation in the Marmara Sea region (Turkey) based on a scenario earthquake. *Tectonophysics*, 391, 357-374

Rangin, C., X. Le Pichon, E. Demirbag, and C. Imren. 2004. Strain localization in the Sea of Marmara: Propagation of the North Anatolian Fault in a now inactive pull-apart, *Tectonics* 23, Art. No. TC2014.

Riepl, J., Bard, P.-Y., Hatzfeld, D., Papaioannou, C. & Nechtschein, S., 1998. Detailed evaluation of site response estimation methods across and along the sedimentary valley of Volvi (EURO-SEISTEST), *Bull. Seismol. Soc. Am.*, 88, 488-502.

Sancio, R.B., Bray, J.D., Steward, J.P., Youd, T.L., Durgunoglu, H.T., Önalp, A., Seed,R.B., Christensen, C., Baturay, M.B. & Karasayilar, T., 2002. Correlation between ground failure and soil conditions in Adapazari, Turkey, *Soil Dynamics and Earthquake Engineering*, 22, 1093-1102.

Sato, T., J. Kasahara, T. Taymaz, M. Ito, A. Kamimura, T. Hayakawa, and O. Tan. 2004. A study of microearthquake seismicity and focal mechanisms within the Sea of Marmara (NW Turkey) using ocean bottom seismometers (OBSs), *Tectonophysics* 391, 303-314.

Somerville, P., Irikura, K., Graves, R., Sawada, S., Wald, D., Abrahamson, N., Iwasaki, Y., Kagawa, T., Smith, N., Kowada, A., 1999. Characterizing crustal earthquake slip models for the prediction of strong ground motion. *Seismol. Res. Lett.* 70, 59–80.

Sørensen, M.B., Oprsal, I., Bonnefoy-Claudet, S., Atakan, K., Mai, M., Pulido, N., Yalciner, C. (in review). Local site effects in Ataköy, Istanbul, Turkey, due to a future large earthquake in the Marmara Sea. Submitted to the *Geophysical Journal International*.

Taymaz, T. et al. 1991. Active tectonics of the north and central Aegean Sea. *Geophysical Journal International*, 106, 433-490.

Tezcan, S.S., Kaya, E., Bal, I.E. and Özdemir, Z., 2002. Seismic amplification at Avcilar, Istanbul, *Engineering Structures*, 24, 661-667.

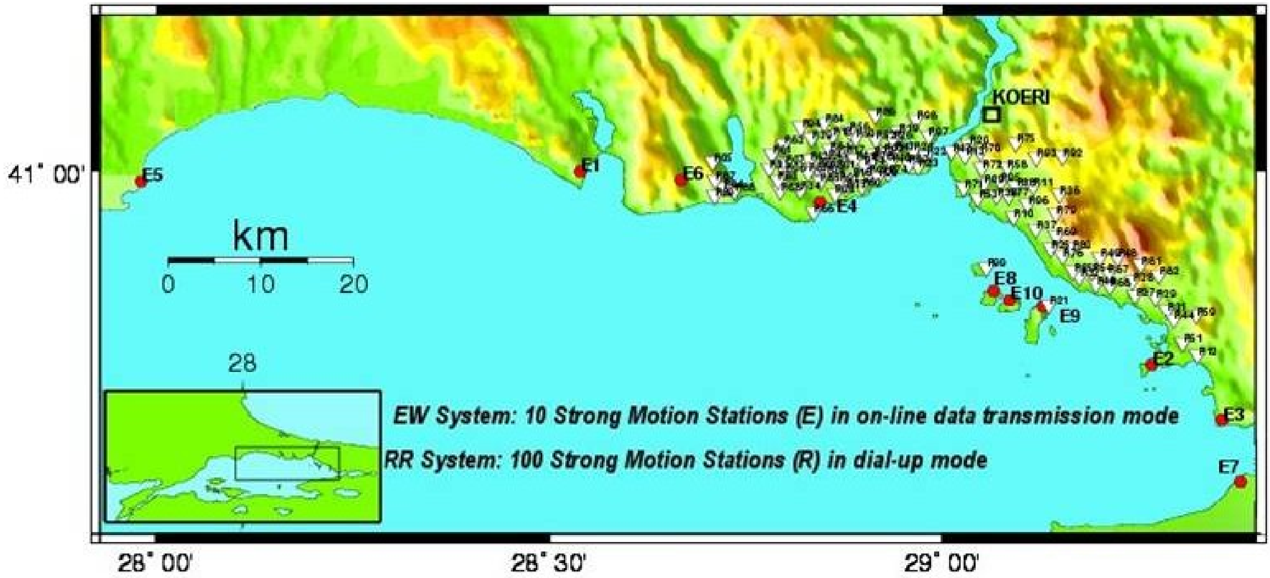

Figure 2.2.1. Istanbul Earthquake Rapid Response and Early Warning System (IERREWS) station locations. White triangles are the Rapid Response System (RRS) stations (From KOERI).

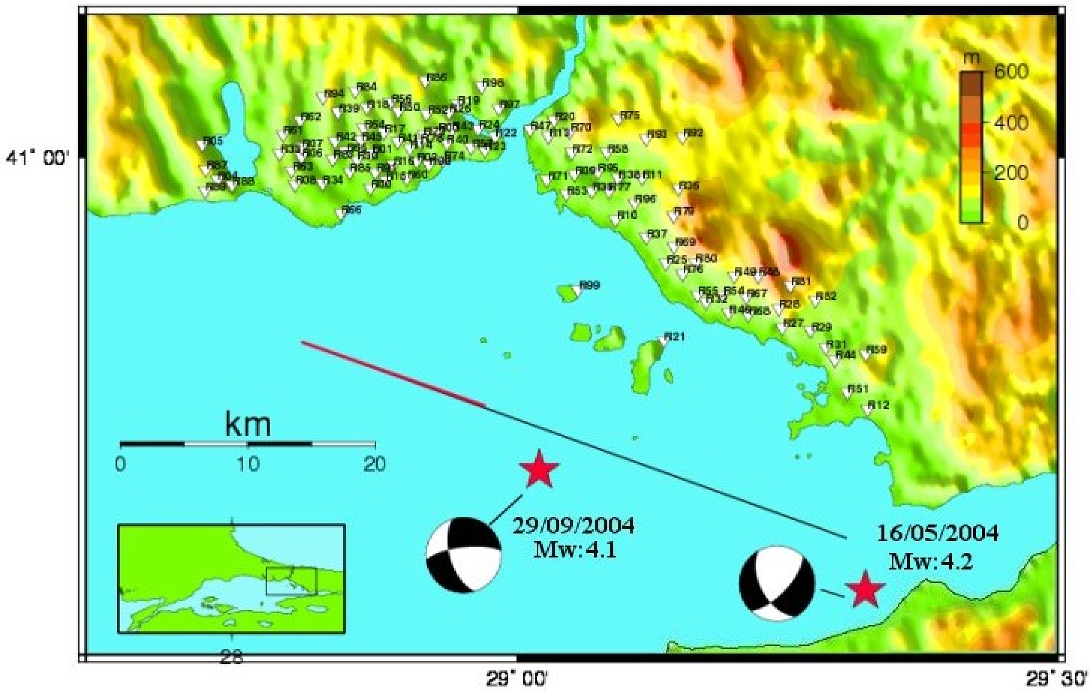

Figure 2.2.2. Locations and focal mechanisms of the two earthquakes recorded by the IEEWRRS are shown together with the approximate location of the North Boundary Fault (NBF). White triangles are the Rapid Response System (RRS) stations. Early Warning stations are not shown for simplicity (From Birgören et al., 2004).

Project No: **EVG1-CT-2002-00069**

Deliverable no. 27 (Partner # 6: UiB)

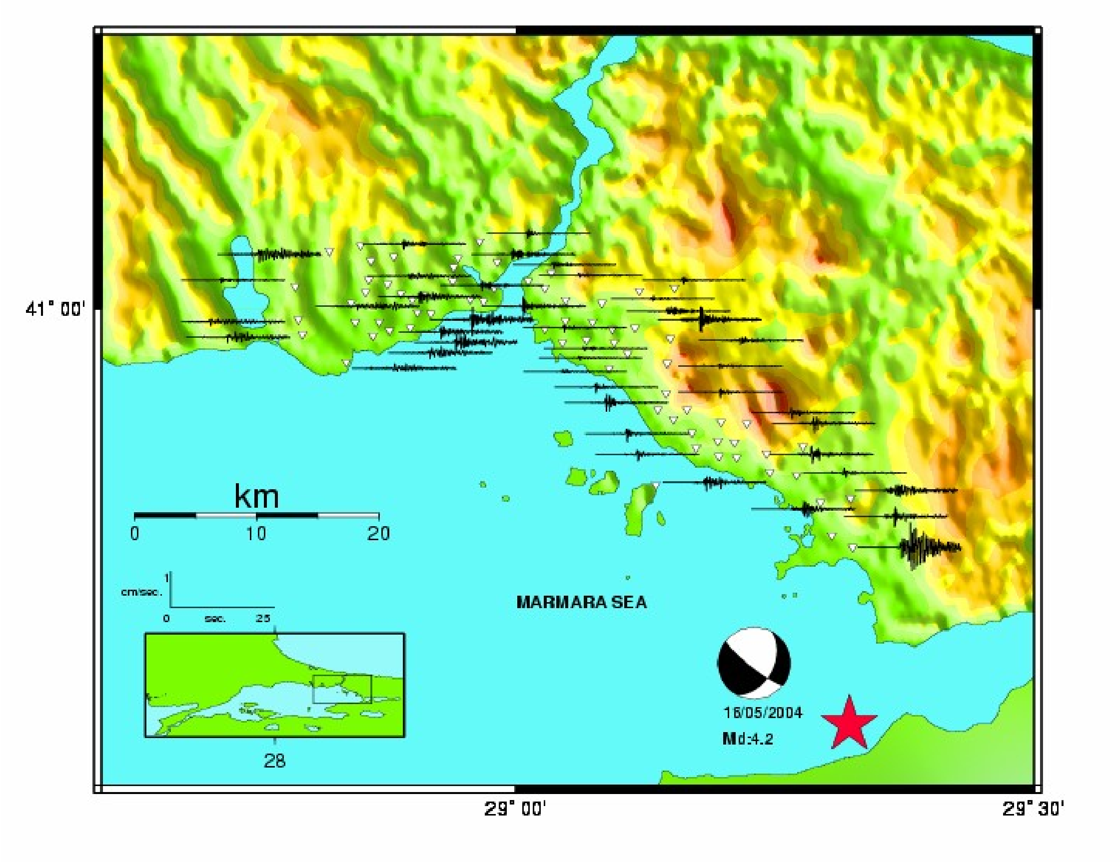

Figure 2.2.3. Accelerograms as recorded by the RRS stations for the earthquake of May 16, 2004 (M_W=4.2). The hypocenter of the event is shown as a red star (from KEORI, UDIM). The focal mechanism indicates an oblique-normal slip which is compatible with the expected motion of the North Boundary fault (From Birgören et al., 2004).

Project No: **EVG1-CT-2002-00069**

Deliverable no. 27 (Partner # 6: UiB)

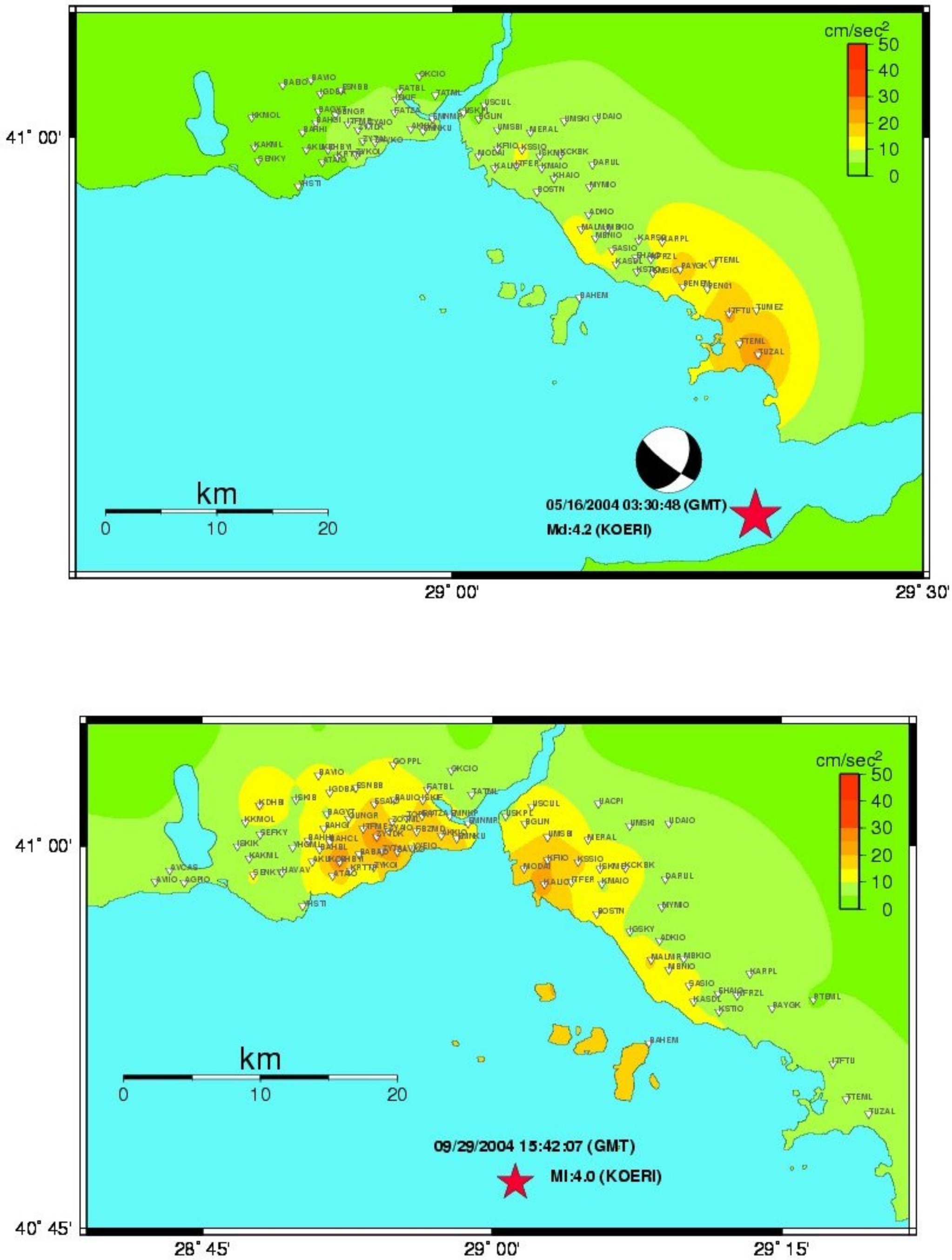

Figure 2.2.4. The distribution of PGA as recorded at the RRS stations for the May 16, 2004 **(top)** and Sept. 29, 2004 **(bottom)** earthquakes. The focal mechanism shown for the May 16, 2004 event indicates an oblique-normal motion compatible with the geometry of the North Boundary fault. (From Birgören et al., 2004)

UNIVERSITAS BERGENSIS

RELIEF

Project No: EVG1-CT-2002-00069

Deliverable no. 27 (Partner # 6: UiB)

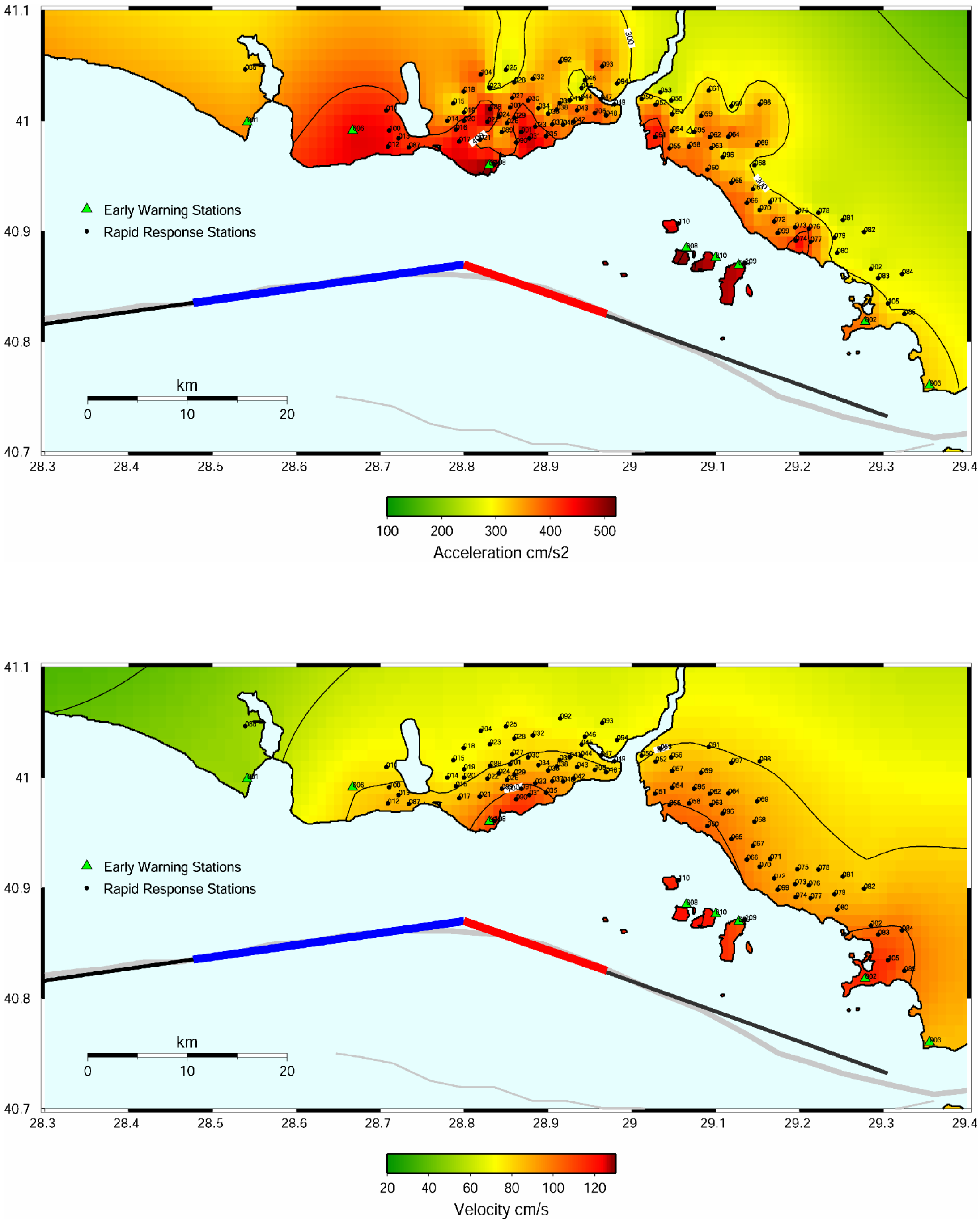

Figure 3.1.1. Ground motion simulation results performed for the RRS station sites. The results are shown in **(top)** peak ground acceleration (PGA) and **(bottom)** peak ground velocity (PGV).

Deliverable no. 27 (Partner # 6: UiB)

Project No: EVG1-CT-2002-00069

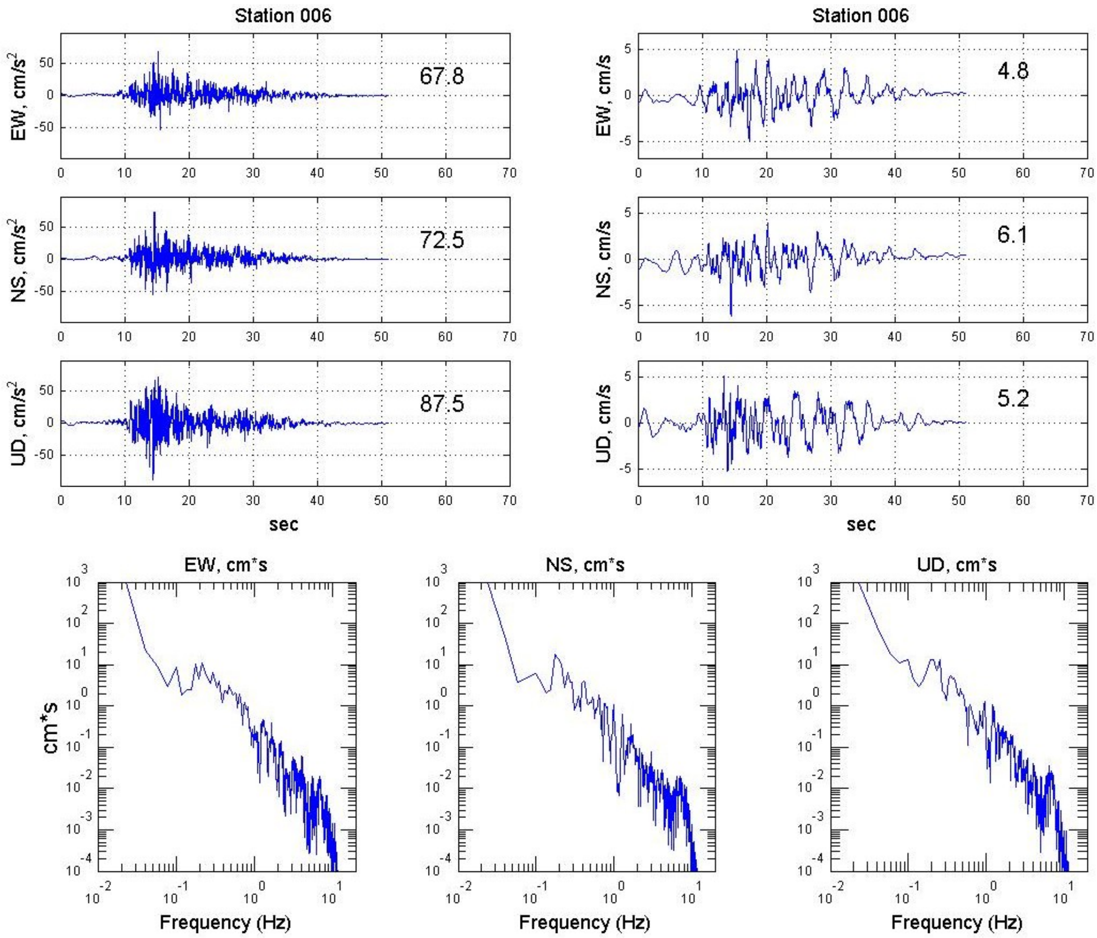

Figure 3.2.1. An example of the simulated ground motions at an RRS station shown in time-series and spectra. Numbers above the waveform give the peak values.

Deliverable no. 27 (Partner # 6: UiB)

Project No: EVG1-CT-2002-00069

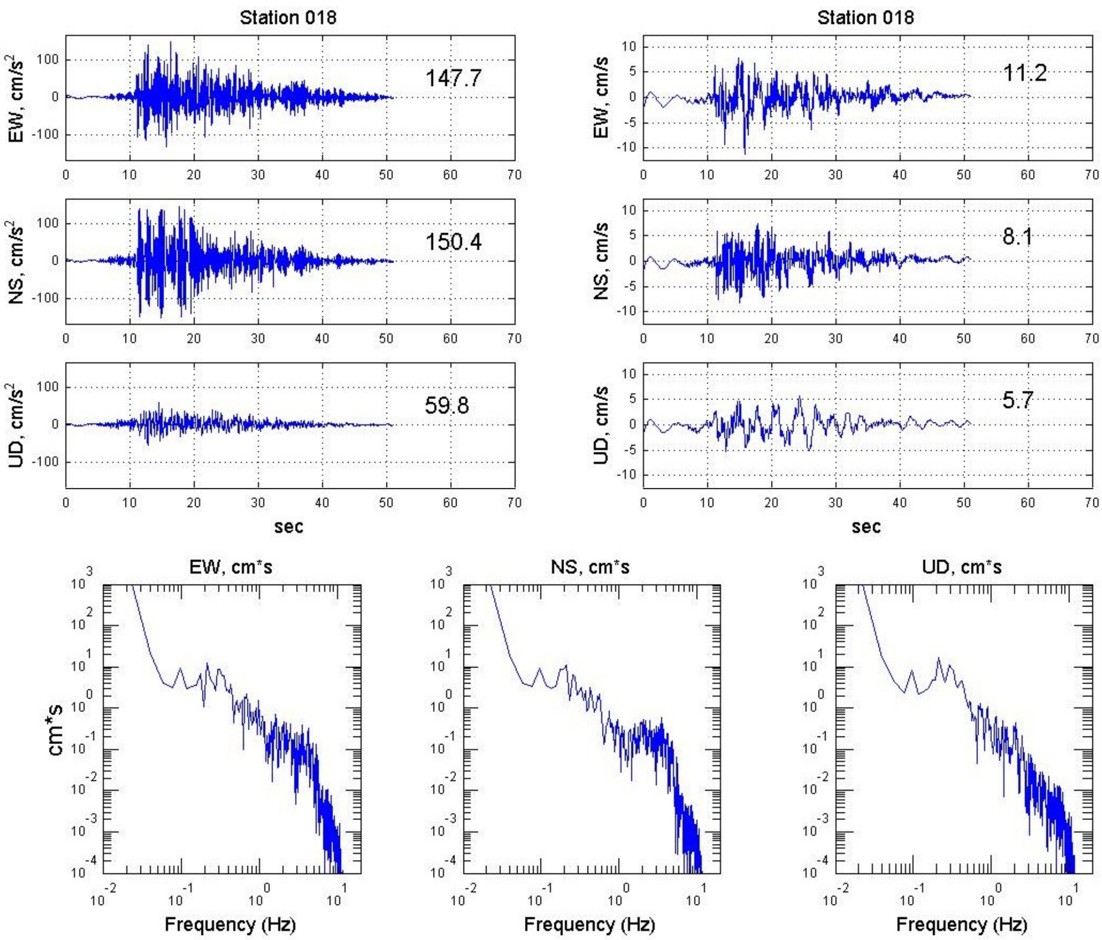

Figure 3.2.2. An example of the simulated ground motions at an RRS station shown in time-series and spectra. Numbers above the waveform give the peak values.

Deliverable no. 27 (Partner # 6: UiB)

Project No: EVG1-CT-2002-00069

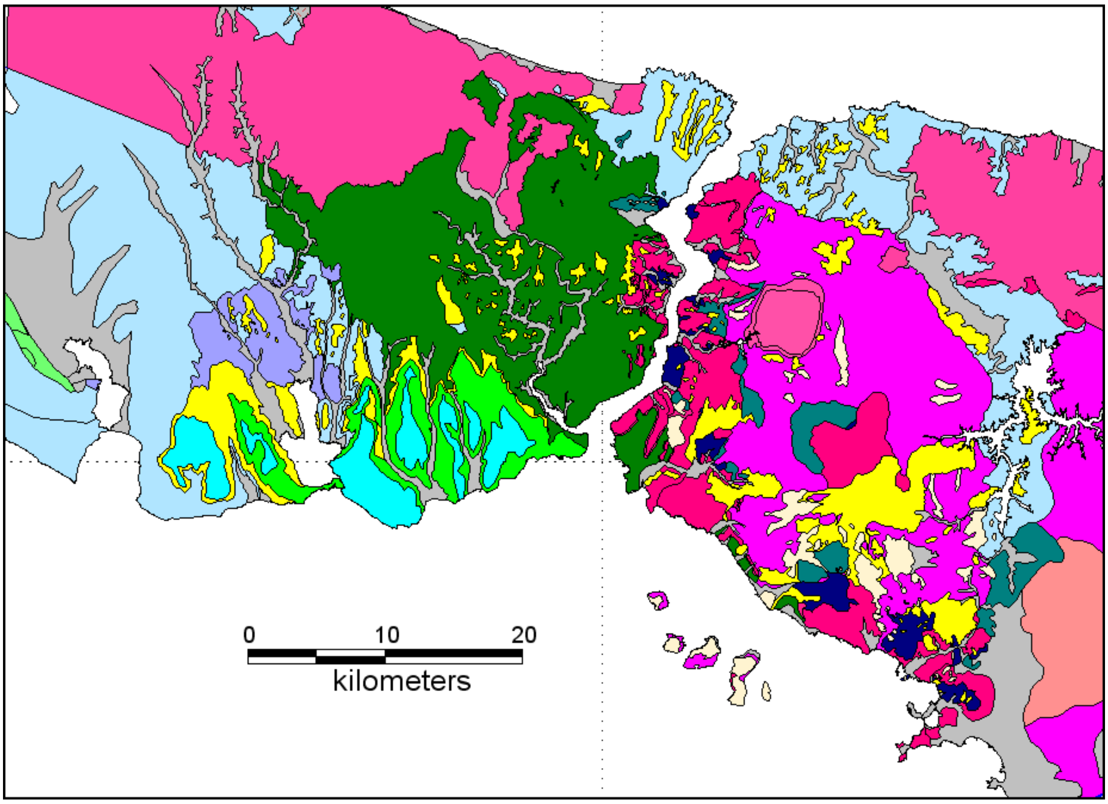

Figure 3.2.3. General geology of the Istanbul region. The legend for the geological units is shown in a separate figure (see next page).

Deliverable no. 27 (Partner # 6: UiB)

Project No: EVG1-CT-2002-00069

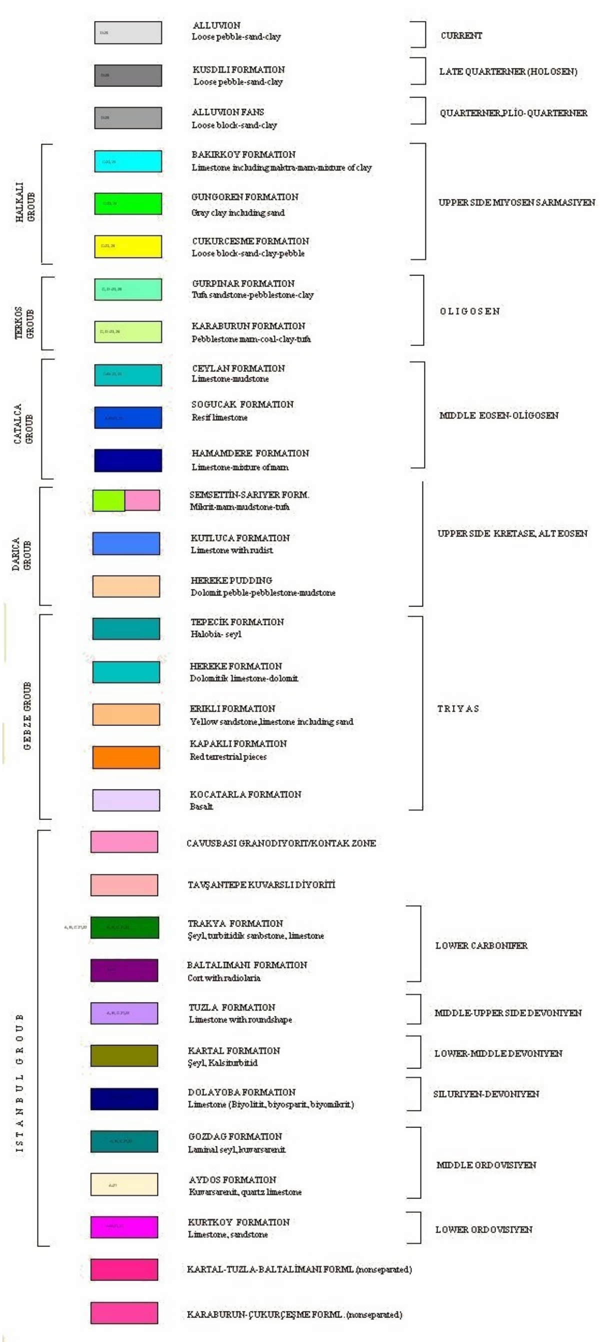

Figure 3.2.3 (continued). The legend for the Geologial map shown in the previous figure.

Deliverable no. 27 (Partner # 6: UiB)

Project No: EVG1-CT-2002-00069

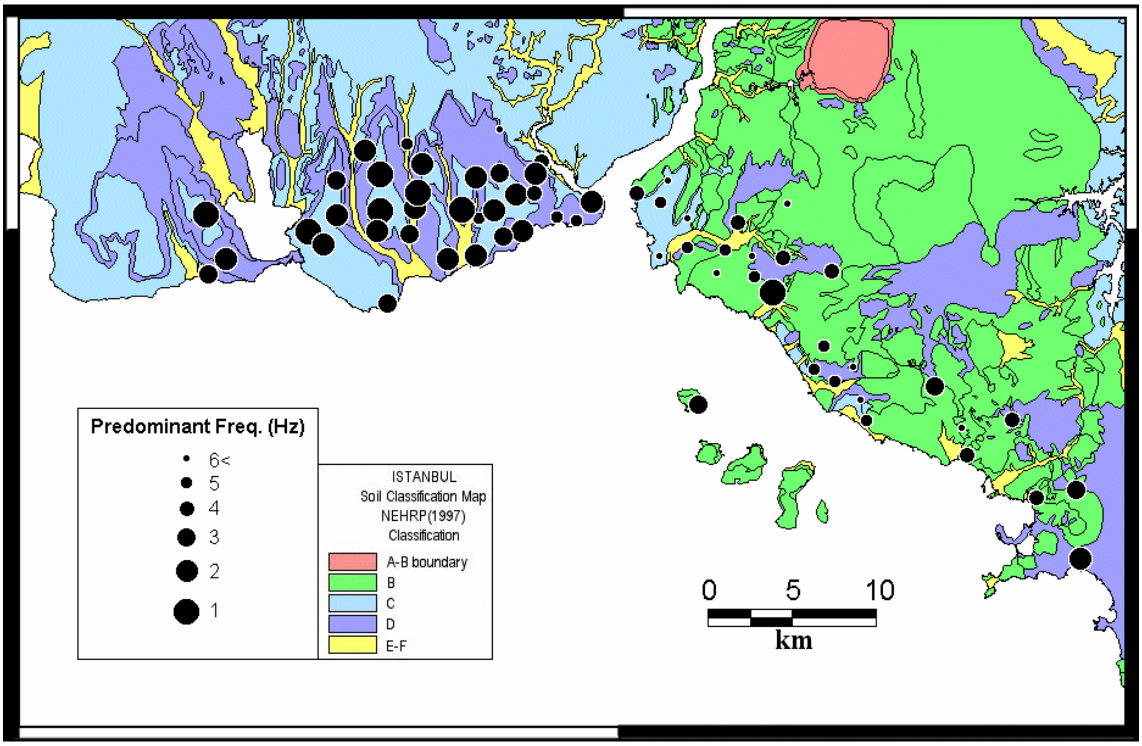

Figure 3.2.4. Predominant frequencies of the RRS sites based on the H/V spectral ratios of the May 16, 2004 and Sept. 29, 2004 earthquake records. Soil classification is based on the NEHRP (1997). Note that the soil classes D, E and F show lower frequencies (From Birgören et al., 2004).

Project No: EVG1-CT-2002-00069

Deliverable no. 27 (Partner # 6: UiB)

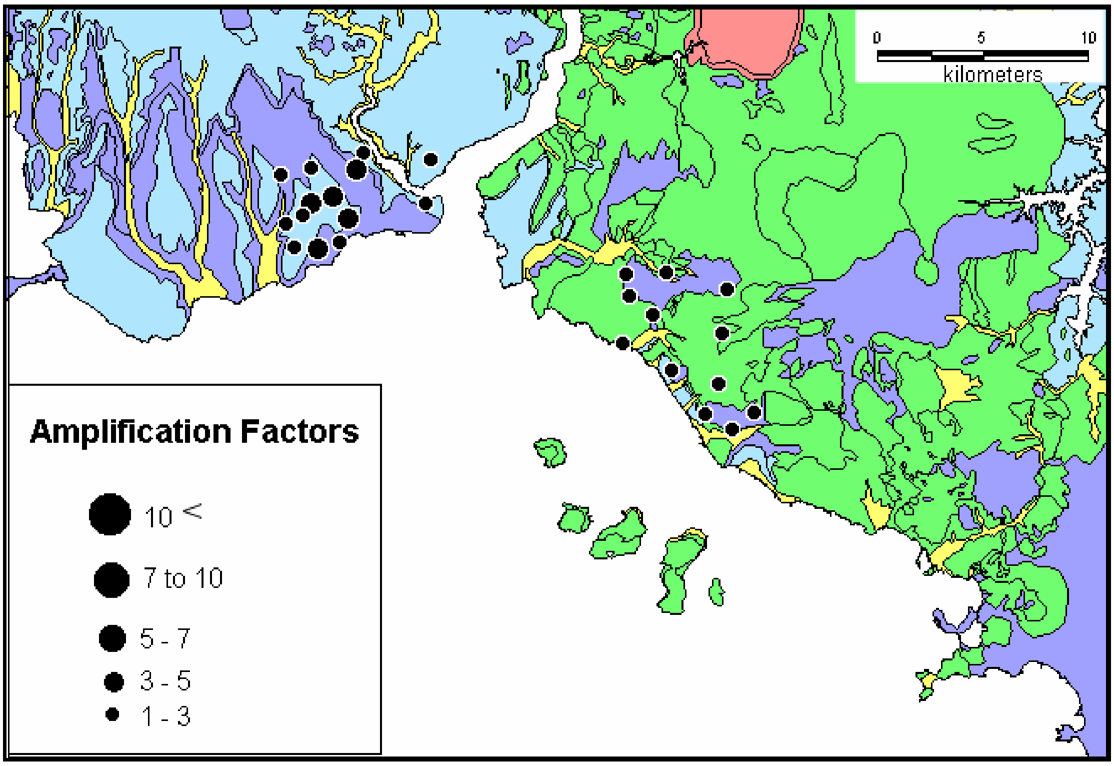

Figure 3.2.5. Map of relative amplification factors for the 1 Hz peaks. Maximum amplifications reach a factor of 5 at the European sites in the NEHRP (1997) soil classes C, D and E. (From Birgören et al., 2004)

Deliverable no. 27 (Partner # 6: UiB)

Project No: EVG1-CT-2002-00069

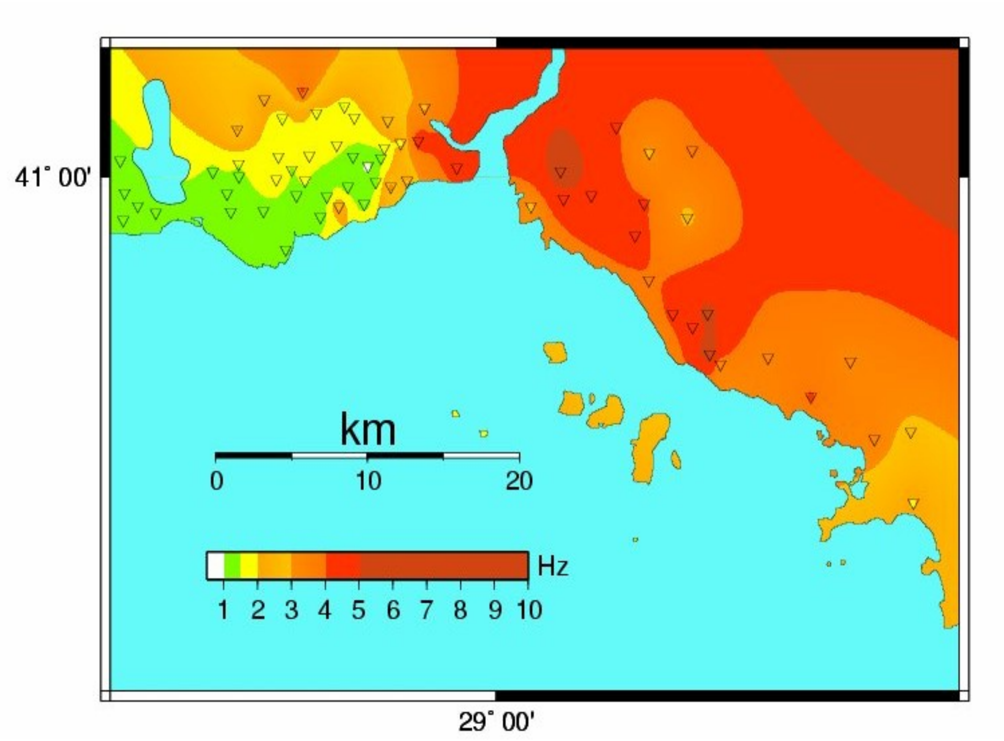

Figure 3.2.6. Contour map of the predominant frequencies as obtained from the H/V spectral ratios of the microtremor measurements. (from Özel et al., 2005).

Deliverable no. 27 (Partner # 6: UiB)

Project No: EVG1-CT-2002-00069

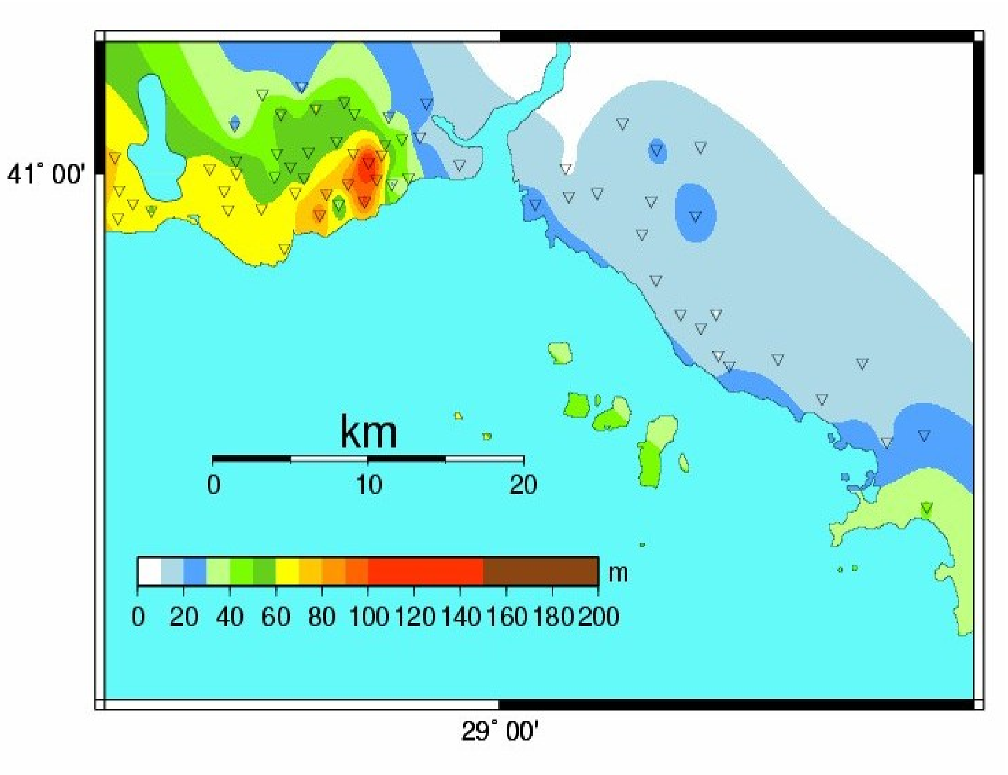

Figure 3.2.7. The soil thickness map based on the empirical relations by Ibs-von Seht and Wohlenberg (1999). (from Özel et al., 2005).

Deliverable no. 27 (Partner # 6: UiB)

Project No: EVG1-CT-2002-00069

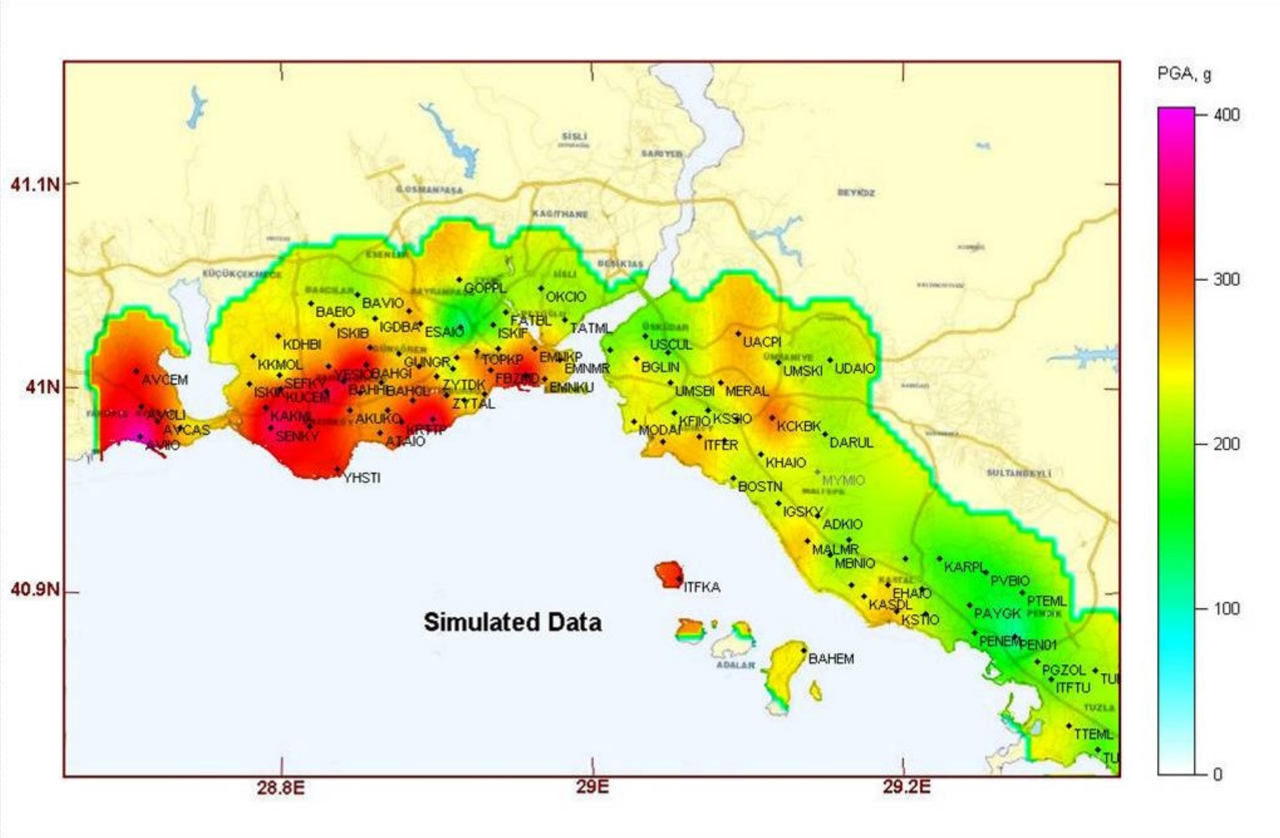

	Figure 4.1. Distribution of the displacement spectra for peak ground accelerations (PGA).	
	Deliverable no. 27 (Partner # 6: UiB)	**Project No: EVG1-CT-2002-00069**

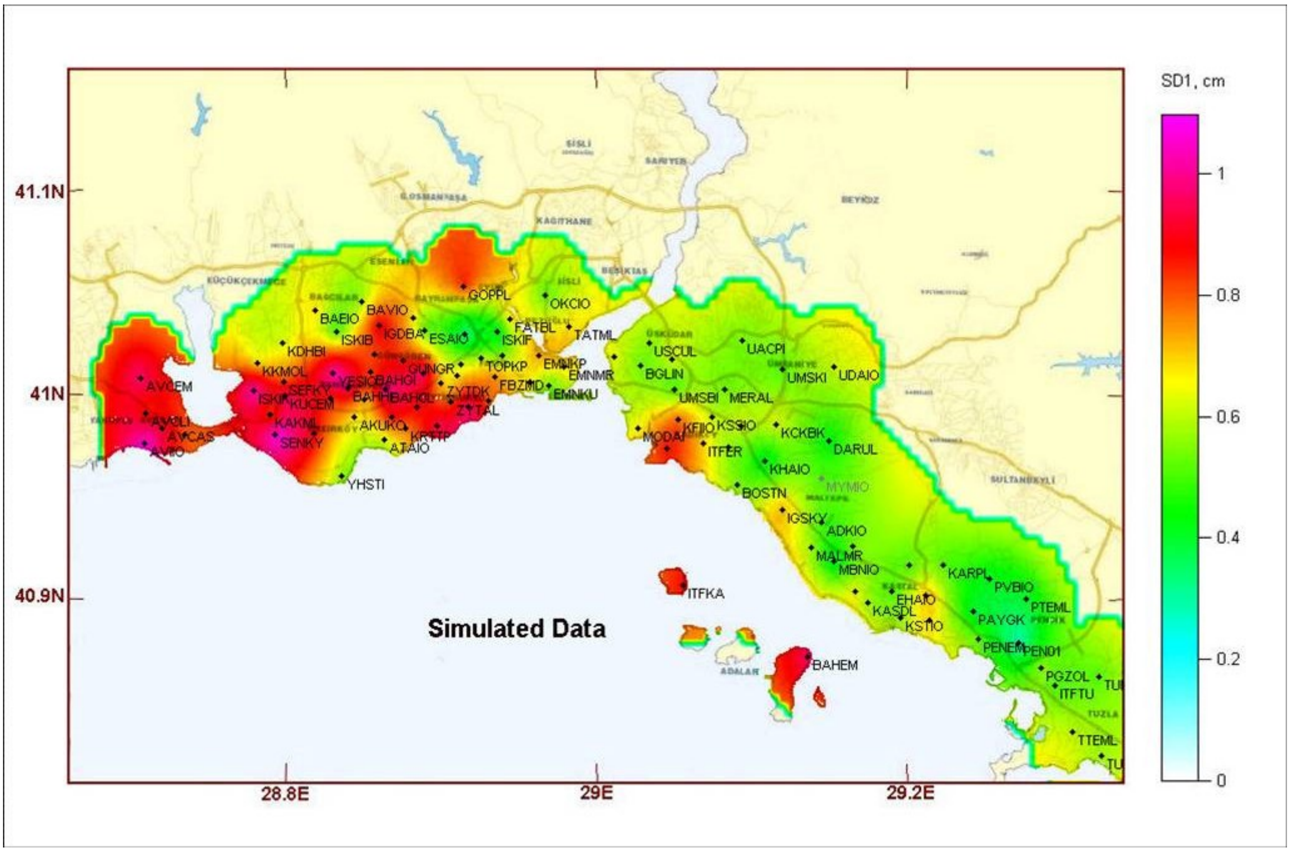

	Figure 4.2. Distribution of the displacement spectra for the frequency range 1-3 Hz (building category "low-rise" 1-4 floors).	
	Deliverable no. 27 (Partner # 6: UiB)	**Project No: EVG1-CT-2002-00069**

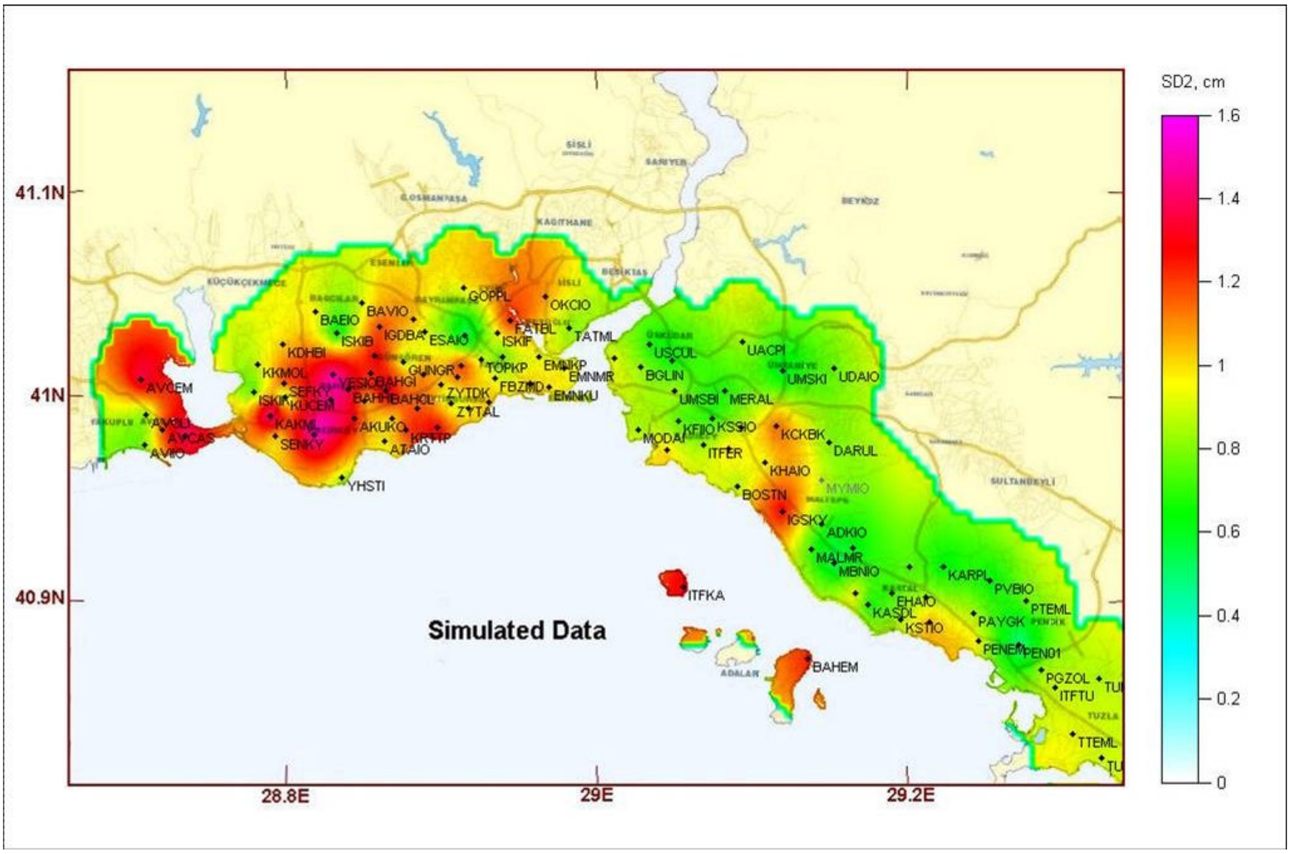

Figure 4.3. Distribution of the displacement spectra for the frequency range 3-5 Hz. Building category "mid-rise" 5-8 floors.

Deliverable no. 27 (Partner # 6: UiB)

Project No: EVG1-CT-2002-00069

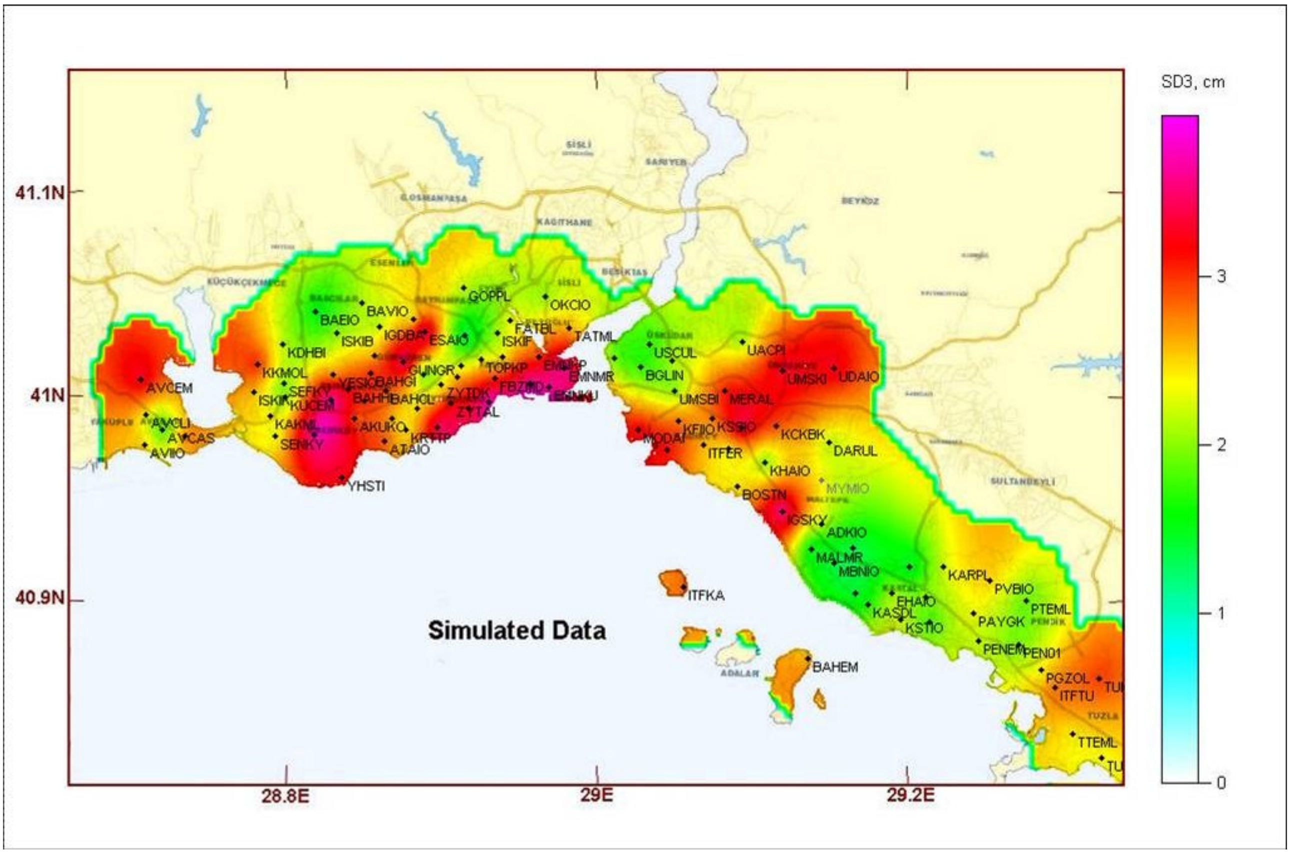

Figure 4.4. Distribution of the displacement spectra for f>5 Hz. Building category "high-rise" >8 floors.

Deliverable no. 27 (Partner # 6: UiB)

Project No: EVG1-CT-2002-00069

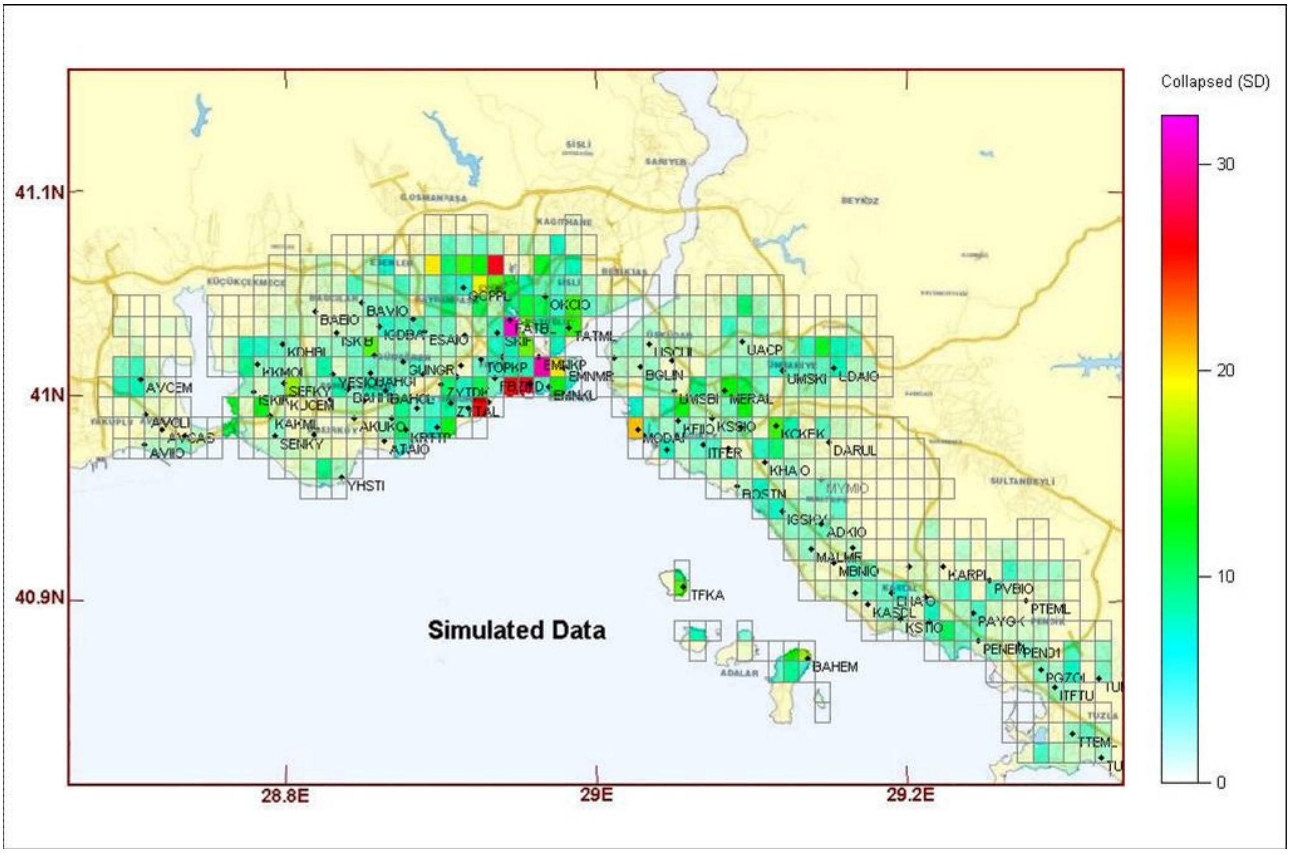

	Figure 4.1.1. The spatial disrtibution of earthquake damage in terms of collapsed buildings.	
	Deliverable no. 27 (Partner # 6: UiB)	**Project No: EVG1-CT-2002-00069**